Entrainment Model Based on Spatio-temporal Impulse Response and Restitution Properties

R. Caulier-Cisterna[1], S. Muñoz-Romero[1,2], A. García-Alberola [3], J. Almendral-Garrote[4], J.L. Rojo-Álvarez [1,2]

[1]Department of Signal Theory and Communications and Telematics and Computation, Rey Juan Carlos University, Fuenlabrada, Madrid, Spain. ({raul.caulier, sergio.munoz, joseluis.rojo }@urjc.es).
[2]Center for Computational Simulation, Universidad Politécnica de Madrid, Spain.
[3]Arrhythmia Unit, Hospital General Universitario Virgen de la Arrixaca, El Palmar, Murcia, Spain. (arcadi@secardiologia.es).
[4] Electrophysiology Laboratory and Arrhythmia Unit, Hospital Monteprincipe, Grupo HM Hospitales, University CEU-San Pablo, Madrid, Spain. (almendral@secardiologia.es).

Resumen

The detailed reaction-diffusion models may be limited in realistic heart-size simulations, appropriately designed cellular automata (CA) can be useful in electrophysiological situations that do not require a detailed microscopic description. We introduce a signal-theory based description of the cell-to-cell impulse propagation, using a space-time impulse response description of the cardiac excitation, in order to extend a previously described CA based on the restitution of intracellular dynamics. In the present work, we show the usefulness of the proposed CA to generate some complex arrhythmia mechanisms and their response to diagnostic stimulation. First, the bipolar electrodes are used to record the simulated extracellular voltage in a normal impulse propagation situation, in order to check the realistic features of the EGM yielded by the model. Second, we created simulations of the entrainment of reentrant arrhythmia in response to programmed electrical stimulation, in order to visualize the shock of their waves, to observe their corresponding EGMs, and to analyze the results. The proposed CA can be a powerful tool for studying the behavior of cardiac arrhythmias.

1. Introduction

Cardioelectric activation models have been widely used for studying the underlying mechanisms of cardiac arrhythmia. Simplified tissue descriptions with cellular automata (CA) were first used [1], which were based on direct connections to the nearest neighbors and on some few possible states for each cell. This provided models with wave propagation, but they did not consider either the curvature effect or the propagation in a partially recovered medium, and more, spiral-waves related to fibrillatory reentrant circuits exhibited a non-physiological angular shape. The second generation of CA [2] modeled the curvature effects by considering squared cell-neighborhoods greater than one element, in such a way that a resting cell was excited when the number of excited cells in the neighborhood exceeded a threshold. The third generation of CA [3] introduced a computationally efficient weighting mask given by a finite-difference approximation to the diffusion operator.

Reaction-diffusion models (RDM) have also been extensively proposed to model the cardioelectric activation. Based on differential equation systems, RDM are capable of reproducing complex phenomena, such as the single myocardial-cell action potential, the impulse propagation through the tissue, or fibrillatory spiral waves [4]. The effect of microscopic variables (e.g., ionic concentrations or individual transmembrane currents) on the macroscopic media can be readily studied with RDM, whereas this is not possible for CA models. RDM can be difficult to use in applications such as realistic heart-size simulations, where the computational burden of RDM precludes their use [5], specially in the study of cardiac electrophysiological situations, which do not require a detailed microscopical description of the dynamics, for instance, some sustained rhythms and reentries [6]. CAs still can be extremely useful in these applications. However, in order to use CAs as a proper nexus between the microscopic and the macroscopic levels, cardioelectric activation properties should emerge naturally from the description and interactions of the model elements.

In a previous work [7], a CA model was proposed overcoming several of these limitations, which still required a noticeable computational burden. In this work, we make it lighter and affordable in some arrhythmia mechanisms and diagnostic therapy with increased complexity. Specifically, we propose to use a linear system theory based description of the cell-to-cell impulse propagation in CA models. This description allows to uncouple the intrinsic charge amount from the extrinsic conduction velocity, by means of a spatio-temporal impulse response used to model the propagation.

2. Methods

The proposed model consists of a 2-dimensional rectangular grid, representing a sheet of tissue, which is divided into elements or pieces accounting for cell groups. The size is

$X \times Y$ cm^2, and the lateral resolution is adjusted to by N elements/cm.

Element Reaction. According to the average state of the membrane channels, each element is described with 3 different states, namely, *rest* (R), *absolute refractory* (AR), and *relative refractory* (RR). Allowed transitions between states are due to depolarization (R to AR), partial repolarization (AR to RR), or total repolarization (RR to R) events. The time instants when transition events occur are calculated from two variables. First, the *Action Potential Duration* (APD), or time interval between a depolarization and its subsequent total repolarization. And second, the *Diastolic Interval* (DI), which is the time interval between a total repolarization and its subsequent depolarization.

The electric restitution curves (see [7]) stand for the behavior of present cycle APD, which is non-linear and increasing with DI at the preceding cycle. The restitution of the conduction velocity is not explicitly considered here. Hence, current APD is dynamically adapted according to previous DI in each element. The relative duration of AR and RR must be determined for each APD, so that $APD = AR + RR$ seconds. In our model, if F denotes the time fraction of APD in AR state, $0 < F < 1$, we have just:

$$AR = F \cdot APD, \quad RR = (1 - F) \cdot APD \tag{1}$$

Note that a state-based description does not provide us with physical levels of instantaneous transmembrane voltage, which should be very convenient for visualization. For this purpose, a single action potential is previously obtained by integration of the Luo-Rudy model [4], providing us with an AP prototype. During the model simulation, this prototype is normalized in time to the APD at each element, and then used as an interpolation look-up table for associating the time elapsed in the present state with the transmembrane voltage level.

Electrical Diffusion. The more neighbors of an element, the easier an element should be depolarized. This corresponds to an extrinsic excitability term to be considered for each element, which is directly related to the myocardial mass. Therefore, depolarization could be modeled as a threshold process, described by an excitation probability P_j^{hom} for each tissue element j in a homogeneous medium, and depending on the simultaneous consideration of intrinsic excitability, given by the conduction velocity (CV), and of the extrinsic excitability (Q), given by the (distance-weighted) number of depolarized neighbors. For model simplicity, we consider a reduction of the influence of a proximal stimulus with the squared distance. The excitability for this element is then

$$P_j^{hom} = K \cdot CV \cdot Q = K \cdot CV \cdot \sum_{i \in N_j} \frac{A_i}{{d_{ij}}^2} \tag{2}$$

where N_j denotes the defined neighborhood of element j; A_i is the binary excitation state (1 excited, 0 elsewhere); and d_{ij} is the distance between i and j element centers. Normalization constant K is fixed in such a way that a flat wavefront propagates at the maximum CV provided by the restitution curve, this is,

$$K = \frac{E[P_j^{hom}]}{CV \cdot E[Q]} \tag{3}$$

where E denotes the expectation operator, $E[P_j^{hom}] = p$ is *a priori* chosen, and it plays a key role to determine the integration time and the average excitation quantity $E[Q]$. Equation (2) represents a spatial impulse response, and it allows us to use signal processing tools, such as bidimensional Fourier transform, to optimize the calculation of the excitation. Moreover, this excitation can be weighted with time to give a spatio-temporal impulse response, hence supporting better the properties of the diffusion process.

For a flat wavefront with constant velocity V propagating longitudinally through a sheet of cardiac tissue with dimensions $L \times W$ cm, sampled at $M = 1/\triangle_s$ samples/cm (where $\triangle_s$ is the dimension of a single cell), a time interval T is needed, this is,

$$T = \frac{L \cdot M \cdot \triangle_s}{CV} \tag{4}$$

where T is related to integration time by $T = N \cdot \triangle_t$ with N an integer whole number. Then, the simulation step time can be calculated as

$$\triangle_t = \frac{L \cdot M}{N} \cdot \frac{\triangle_s}{CV} \tag{5}$$

therefore, the total number of excited cells in $\triangle_t$ is $L \cdot W \cdot M^2/N$. Moreover, for a flat wavefront and a neighborhood with $R = 1$, the maximum number of excited cells becomes $M \cdot W$, so that the average excitability probability p is then

$$p = \frac{L \cdot W \cdot M^2/N}{M \cdot W} = \frac{L \cdot M}{N} \tag{6}$$

Introducing this relationship in Eq. (5), it gives

$$\triangle_t = p \cdot \frac{\triangle_s}{CV} \tag{7}$$

where it is clearly shown the direct relationship between time step and p. The dependence between the value p and $E[Q]$ has still to be checked. Choosing $p = 1$, the wavefront covers $\triangle_s$ in $\triangle_t$ so the neighborhood for a single cell is up to three excited cells and then $E[Q] = Q_{max}/3$. For the case $p = 2$, the wavefront covers a column in twice $\triangle_t$, and consequently, $E[Q]$ is expected to be bigger than the previous case, in fact, it can be shown that $E[Q] = Q_{max}/2$.

This expression can be easily extended to a heterogeneous substrate. If CV_l denotes the mean longitudinal conduction velocity along a fiber, and CV_t denotes the transversal conduction velocity among proximal fibers, then:

$$P_j^{het} = K \cdot \left(CV_l \sum_{i \in NL_j} \frac{A_i}{{d_{ij}}^2} + CV_t \sum_{i \in NT_j} \frac{A_i}{{d_{ij}}^2} \right) \tag{8}$$

where NL_j, NT_j are the subsets of neighbors along the longitudinal and transversal directions, respectively.

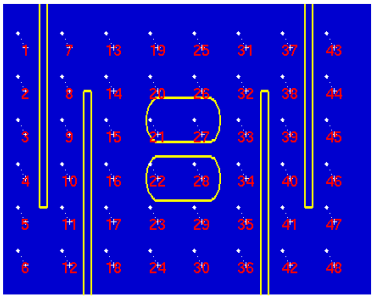

Figura 1. *Simulated cardiac tissue. Corridors are generated with blocked regions, so that the impulse will follow the corridor path. An infarcted region in the middle of the tissue protects a slow conduction way, in an eight-figure mechanism.*

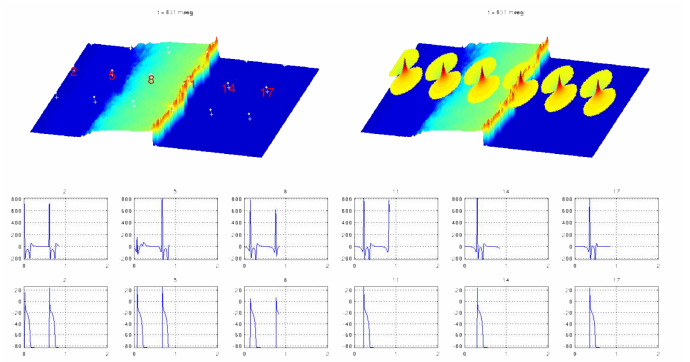

Figura 2. *EGM recording in the central electrodes of the simulated cardiac tissue. The scope of bipolar electrodes can be seen in yellow, with their corresponding EGMs and the action potential below them.*

3. Results

In this section, we first present the results of a simulation with the proposed CA on a plane wavefront, and then, a specific application is built, namely, the entrainment used in electrophysiological studies to help the clinician to localize the arrhythmia anatomical origin. Our CA was previously used in [8] to provide with detailed simulations on the entrainment technique, and in this work we only present the technical details, and a different example.

3.1. Plane Wavefront

Tissue Model. Several tissue models can be used in the CA. From an electrophysiological point of view, a two-dimensional cardiac tissue model can be made, including slow conduction pathways, corridors, and infarcted regions. Corridors are used to extend the distance between the cardiac tissue and the pacing electrodes, without a need for creating extremely large tissue models. Moreover, unipolar and bipolar electrodes can be put in the desired position over the tissue, in order to record the extracellular potential and to visualize the EGMs. Figure 1 depicts a 2×5-cm^2 cardiac tissue model with 48 bipolar electrode pairs. The slow conduction pathway in the middle of the infarcted regions is given a CV $50\,\%$ slower.

EGM Catchment Model. Both unipolar and bipolar electrodes are placed on the cardiac tissue at a vertical distance, which is adjusted to provide with EGMs with similar shape to the observed in the electrophysiological studies (in this simulation, $0{,}1$ cm). Figure 2 shows the recording of bipolar electrode configuration along a cardiac tissue centered line. Panels in the middle row shows the recorded EGM and the action potentials below these electrodes.

Simulation Visualization. The results of the CA simulations can be readily seen on a video generated by post-processing of the data stored in Matlab®. These data are also used for subsequent analysis, such as activation time maps generation of RR-peak detection.

3.2. Aplication to Entrainment

Thanks to the usefulness and user-friendly design of the CA, it can be used as research tool for a variety of pathologies, as well as a teaching tool. We show next an application to the modeling of entrainment in reentrant circuits.

Under normal conditions, the electric impulse is generated in the sinus node and it drives the activation of atria and ventricles. However, in some cases, the electrical activation can persist without extinguishing in a cardiac region, over some time enough to its neighbor tissue can recover its excitability (and hence overcome the refractory period), so that the same impulse is able to excite again (totally or partially) the heart again. This is called reentrant stimulus, and it is the mechanism for cardiac reentry. The path followed by the driving impulse until exciting again the tissue previously recovered is called reentry circuit.

In the electrophysiological studies, arrhythmia are often treated, and controlled stimulation techniques are often used, such as the entrainment techniques. These last consist of the acceleration of a tachycardia up to the same cardiac frequency in which a stimulus train is applied, due to the continuous reentry with each paced stimulus of the train [9]. In the case of reentry-originated tachycardia, each stimulus in the train enters the circuit and it propagates in two directions, namely, the antidromic front shocks with the wavefront around the circuit, whereas the ortodromic front advances the next beat of the tachycardia. When the over-stimulation is stopped, the tachycardia must continue without relevant changes in its morphology and cycle length, to consider that entrainment has been produced.

Figure 3 shows the results for an example of entrainment simulated with the CA. In a 3×3-cm^2 tissue with an eight-figure in the center, up to 45 bipolar electrodes are placed at $0{,}1$ mm height. An impulse was delivered in this tissue which generated a reentrant circuit at 540-ms cycle-lenght, as seen in the EGMs of the figure. Then, from a point in the lower side of the cardiac tissue, an impulse was generated at 480-ms cycle-length to capture the reentring circuit, panel (a). In panel (b), the isochronal map is depicted, showing the collision of the antidromic front with the reentrant circuit front, whereas the antidromic front is advanced to the next tachycardia beat, hence capturing the reentring circuit. When the over-stimulation stops, the tachycardia continues without changing its morphology or cycle length, as seen in panel (d). Therefore, the simulation has generated an entrainment in a reentring circuit.

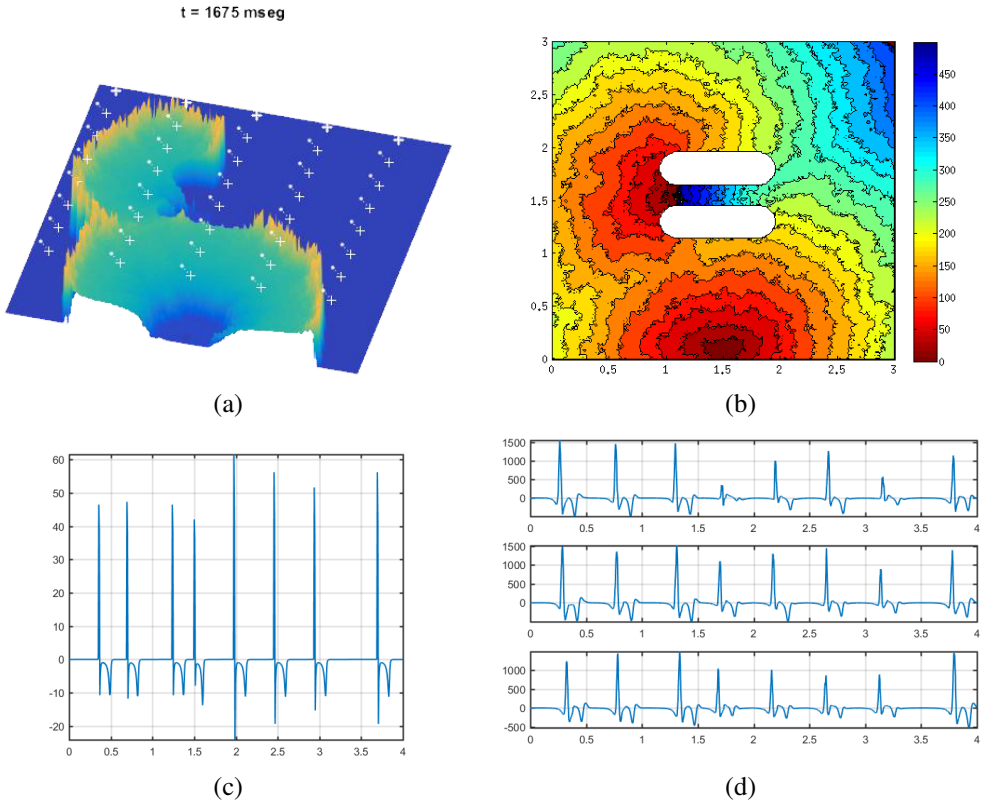

Figura 3. *Results on entrainment modeling: (a) Video generated with the proposed CA. (b) Corresponding isochronal map for entrainment; (c) Reference EGM for the isochronal map; (d) EGMs of bipolars electrodes catchment.*

4. Conclusion

In the present work, we have suported the use of CA in the investigation of the cardiac arrhythmias that are studied in electrophysiology. It is important to know the behavior of these arrhythmias and how to locate them within the heart in a fast and accurate way, thus making the electrophysiological studies shorter in time and improving the precision in the detection for the ablation of these arrhythmias. Using these CAs allows more accurate knowledge of the behavior of the arrhythmias, allowing their effective localization and control in controlled stimulation studies, as it was the case study performed in this work.

Acknowledgments

This work was partially supported by Research Grants PRINCIPIAS, FINALE, and KERMES (TEC2013-48439-C4-1-R, TEC2016-75161-C2-1-R, and TEC2016-81900-REDT) from Spanish Government.

Referencias

[1] G. K. Moe, W. C. Rheinboldt, and J. A. Abildskov, "A computer model of atrial fibrillation," *American Journal of Heart*, vol. 67, pp. 200–20, Feb. 1964.

[2] M. Gerhardt, H. Schuster, and J. J. Tyson, "A cellular automation model of excitable media including curvature and dispersion," *Science*, vol. 247, pp. 1563–1566, March 1990.

[3] J. R. Weimar, J. J. Tyson, and L. T. Watson, "Diffusion and wave propagation in cellular automaton models of excitable media," *Physica D: Nonlinear Phenomena*, vol. 55, no. 3-4, pp. 309–327, 1992.

[4] Y. Rudy and W. L. Quan, "A model study of the effects of the discrete cellular structure on electrical propagation in cardiac tissue.," *Circulation Research*, vol. 61, no. 6, pp. 815–823, 1987.

[5] F. B. Sachse, *Computational Cardiology: Modeling Of Anatomy, Electrophysiology, And Mechanics*. Springer-Verlag, New York Inc, 2004.

[6] P. Hammer, D. Brooks, and J. Triedman, "Entrainment response in a model of reentrant tachycardia," in *Computers in Cardiology 2001*, pp. 229–232, IEEE, 2001.

[7] F. A. Atienza, J. R. Carrión, A. G. Alberola, J. L. R. Álvarez, J. J. S. Muñoz, J. M. Sánchez, and M. V. Chávarri, "A probabilistic model of cardiac electrical activity based on a cellular automata system," *Revista Española de Cardiología (English Edition)*, vol. 58, no. 1, pp. 41–47, 2005.

[8] J. Almendral, R. Caulier-Cisterna, and J. L. Rojo-Álvarez, "Resetting and entrainment of reentrant arrhythmias: part i: concepts, recognition, and protocol for evaluation: surface ecg versus intracardiac recordings," *Pacing and Clinical Electrophysiology*, vol. 36, no. 4, pp. 508–532, 2013.

[9] B. Waldecker, J. Coromilas, A. E. Saltman, S. M. Dillon, and A. L. Wit, "Overdrive stimulation of functional reentrant circuits causing ventricular tachycardia in the infarcted canine heart. resetting and entrainment.," *Circulation*, vol. 87, no. 4, pp. 1286–1305, 1993.